Journal of Applied Polymer Science

Synthesis, characterization, metal sorption, and biological activity of poly(*N*-heterocylic acrylamide)

Othman A. Al-Fulaij, Abdel-Zaher A. Elassar, Ahmed F. El-asmy
Chemistry Department, Faculty of Science, Kuwait University, P.O.B 5969-Safat 13060, Kuwait
Correspondence to: A.-Z. A. Elassar (E-mail: aelassar@yahoo.com)

ABSTRACT: *N*-heterocyclic acrylamide monomers were prepared and then transferred to the corresponding polymers to be used as an efficient chelating agent. Polymers reacted with metal nitrate salts (Cu^{2+}, Pb^{2+}, Mg^{2+}, Cd^{2+}, Ni^{2+}, Co^{2+}, Fe^{2+}) at 150°C to give metal-polymer complexes. The selectivity of the metal ions using prepared polymers from an aqueous mixture containing different metal ion sreflected that the polymer having thiazolyl moiety more selective than that containing imidazolyl or pyridinyl moieties. Ion selectivity of poly[*N*-(benzo[d]thiazol-2-yl)acrylamide] showed higher selectivity to many ions e.g. Fe^{3+}, Pb^{2+}, Cd^{2+}, Ni^{2+}, and Cu^{2+}. While, that of poly[*N*-(pyridin-4-yl)acrylamide] is found to be high selective to Fe^{3+} and Cu^{2+} only. Energy dispersive spectroscopy measurements, morphology of the polymers and their metallopolymer complexes, thermal analysis and antimicrobial activity were studied. © 2015 Wiley Periodicals, Inc. J. Appl. Polym. Sci. **2015**, *132*, 42712.

KEYWORDS: biomaterials; morphology; polyamides; synthesis and processing

Received 9 April 2015; accepted 10 July 2015
DOI: 10.1002/app.42712

INTRODUCTION

Polymers containing aromatic, heterocyclic or heteroaromatic systems comprise an interesting class of polymers because of their significant environmental,[1–3] biological,[4–6] and pharmacological uses.[7–10] Many efforts have been done for the synthesis of polymers containing heterocyclic moiety. The presence of heterocyclic moiety in the polymeric chain acts as a good chelating ligand for medicinal[11–15] and analytical applications.[16–20] Generally, the formation of polymer complex is depending on (1) backbone of the polymeric chain, (2) function groups, (3) pH, and (4) distance between pendant ligand and backbone.

Heavy metal pollution is spreading throughout the world with the expansion of industrial activities. In other words, heavy metals which are of great environmental concern must be removed. Industrial wastewater contains high levels of heavy metals and to avoid water pollution, treatment is needed before disposal. Removal of metals from wastewater is achieved principally by the application of several processes of adsorption, sedimentation, electrochemical processes, ion exchange, biological operations, cementation, filtration and membrane processes, chemical precipitation, and solvent extraction. Adsorption is an important procedure for the removal of heavy metals from the environment. The main properties of the adsorbents for heavy metal removal are strong affinities and high loading capacity.

In this article and in continuation of the previous studies[21–24] we are aimed to prepare and develop the ability of a polymeric material to be used in waste treatment. In other words, increases the efficiency to metal uptake from an aqueous medium. We are believed that the heterocyclic moiety in the polymeric chain can force the metal uptake so that we are directed to use different heterocyclic amine with π-deficient and π-excessive systems to prepare different monomeric materials. On the other hand, the presences of the heterocyclic moiety containing dentate atoms (N, O, and S) are expected to increase the metal uptake efficiency. In addition, the biological and medicinal activities of different heterocyclic moieties and their metal complexes are responsible for the extensive work on this field.

The investigation of monomers, polymers and metal polymer complexes in bioactivity studies are another goal. Elemental analysis, IR, NMR, MS, EDS, and thermal measurements were utilized to characterize the synthesized monomers, polymers, and metal polymer complexes.

EXPERIMENTAL

Materials

4-Aminopyridine, 2-aminobenzimidazole, 2-aminobenzthiazole, acryloyl chloride, ammonium hydrogen carbonate (Aldrich) were used as received. All metal salts and other chemicals were reagent grade and used without further purification.

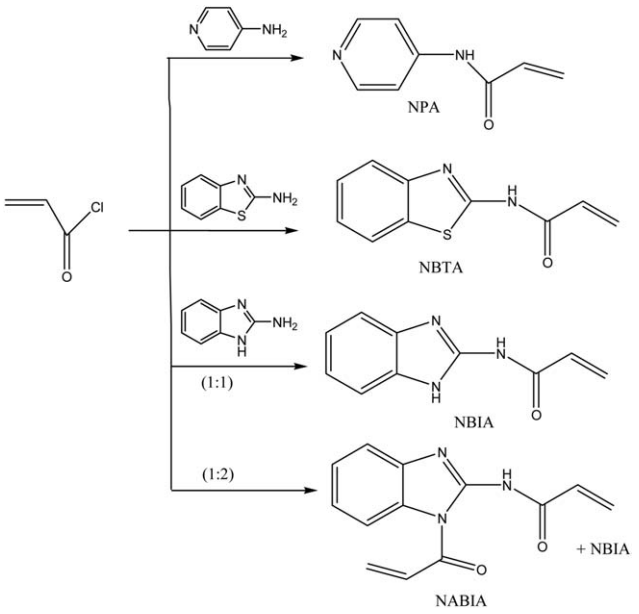

Scheme 1. Synthesis of monomers.

Physical Measurements

Elemental analyses were performed at Analab, on LECO CHNS–932, Faculty of Science, Kuwait University. The IR spectra were recorded as KBr discs for the monomers, polymers, and the metal polymer complexes on Perkin-Elmer 2000 FT IR Spectrophotometer (Kyoto, Japan). The (^{1}H and ^{13}C) NMR spectra were recorded on a Bruker DPX 400, 400 MHz superconducting NMR Spectrometer in DMSO-$d_6$as solvent andTMS as an internal standard; the chemical shifts are reported in δ units (ppm).Scanning Electron Microscopy (SEM) for the polymers and their metal polymer complexes were examined at room temperature (25°C) in a model JSM 6300 JEOL scanning electron microscope (Akishima, Japan) at 20 kV. TGA was carried out in nitrogen using a Schimadzu DSC 50 analyzer (Japan) set at a heating rate of 10°C/min and the temperature range 25–800°C. Energy Dispersive Spectroscopy (EDS) chemical area mapping the metal polymer complexes was performed with

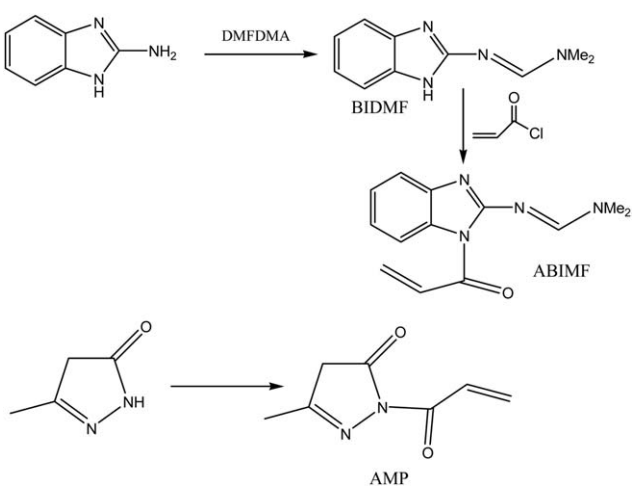

Scheme 2. Synthesis of ABIMF and AMP monomers.

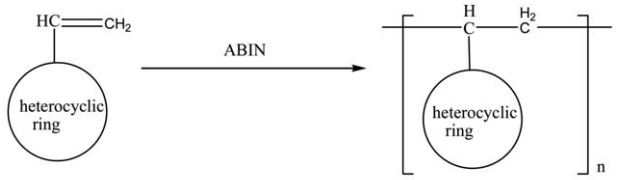

Heterocyclic ring = 4-pyridyl, 2-benzoimidazolyl, 2-benzothiazolyl, pyrazolyl

Scheme 3. Preparation of polymer.

LINK'S exl II energy dispersive Spectrometer (Oxford instruments, Analytical, Hywycombe, Bucks, and UK) attached to the scanning electron microscope to measure the absorbed ions from solution.Mass spectra were recorded on GS/MS INCOS XL Finnigan MAT.

Synthesis of Monomers, Polymers, and Metal Polymer Complexes

Synthesis of Monomers. *N-(pyridin-4-yl)acrylamide (NPA); N-(benzo[d]thiazol-2-yl)acrylamide (NBTA); N-(1H-benzo-[d] imidazole-2-yl)acrylamide (NBIA);N-(1-acryloyl-1H-benzo-[d] imidazole-2-yl)acrylamide (NABIA) and 1-acryloyl-3-methyl-1H-pyrazol-5(4H)-one (AMP)*

The above monomers were prepared by adding ice-cold solution (0°C) of 4-aminopyridine, 2-aminobenzthiazole, 2-aminobenzimidazole or 3-methyl-1H-pyrazol-5(4H)-one (0.01 mol) in acetone to ice-cold solution of acryloyl chloride (0.015 mol) in same solvent (30 mL) drop-wise in 30–40 min. The reaction mixture was left at 0°C overnight in the fridge and then neutralized with ammonium bicarbonate. The solid product was collected by filtration, washed with iced water (200 mL) and crystallized from MeOH or EtOH.

Synthesis of Polymers. *Poly-N-(pyridin-4-yl)acrylamide (PNPA); Poly-N-(benzo[d]thiazol-2-yl)acrylamide (PNBTA); Poly-N-(1H-benzo-[d]imidazole-2-yl) acrylamide (PNBIA) and Poly-1-acryloyl-3-methyl-1H-pyrazol-5(4H)-one (PAMP)*

The above polymers were synthesized via heating a solution of monomers in DMF in the presence of catalytic amount of AIBN for 5 h on the water bath at 75°C. The polymer was collected by evaporation in evaporating dish or after cooling and treating with ethanol : water (1 : 2 v/v) a mixture. The solid product was filtered out and washed with cold ethanol. For purification, the solid product was heated under reflux in ethanol for 1 h and then filtered and dried at 50°C under a reduced pressure for 48 h.

Synthesis of Metal Polymer Complexes. A filtered solution of metal nitrate (0.01 mol) was added to a suspension of polymer (0.50 g) in DMF. The reaction mixture was heated under reflux for 5 h. The solid product formed into evaporation of the solvent under a vacuum was collected by filtration and then washed by diethyl ether. The complex was purified by heating in ether or ethanol for 30 min and then filtered to collect pure solid complex.

Table I. Elemental Analysis and Mass Spectra of the Prepared Compounds

Cpd No.	MS (*m*/*z*)	Elemental analysis found/calcd C	H	N	S
NPA	148.0 (4%), 94.1 (100%), 55.0 (18%)	65.01	5.31	19.21	
		64.85	5.44	18.91	
NBTA	204.1 (42%), 176.1 (100%), 150.1 (28%), 55.1 (14%)	59.11	4.01	14.00	15.85
		58.80	3.95	13.72	15.70
NBIA	187.1 (60%), 133.1, 105.1, 69.1, 55.1	64.22	5.12	22.65	
		64.16	4.85	22.45	
NABIA	241.1 (60%), 133.1, 105.1, 69.1, 55.1	64.56	4.52	17.63	
		64.72	4.60	17.42	
ABIMF	242.12 (15%), 188.1, 172.1, 55.1	64.66	6.01	23.23	
		64.45	5.82	23.13	
BIDMF	188.10 (23%), 144.1, 117.0, 71.2	64.00	6.31	30.02	
		63.81	6.43	29.77	

Ion Selectivity

To an aqueous solution of the metal nitrate mixture (Pb^{2+}, Cu^{2+}, Fe^{3+}, Cd^{2+}, and Ni^{2+}), PNBTA, PNPA, or PNBIA (0.5 g) were added. The pH was adjusted to the range of 6–8. The mixture was left for 24 h without stirring. The reaction product was filtered and the metal content remaining in the filtrate was measured by atomic absorption spectra (AAS).

Determination of Metal Ions in Water Samples

Twenty liters of a real sample of Gulf water were preconcentrated to a final volume of 160 mL. The metal ion concentration was determined by ICP-OES. About 150 mL of the preconcentrated sample was divided into three portions of 50.0 mL and then treated with 0.50 g of PNBTA with shaking rates of 350 rpm for 24 h. The mixture was filtered and the polymer washed several times with doubly distilled water. The results of ICP-OES measurements before and after treatments and the metal uptake % onto the chelating polymer were computed according to the following equation:

$$\%\ \text{sorption} = \left[C_i - C_f / C_i\right] \times 100$$

where C_i and C_f are the initial and final concentrations of the metal ion (mg/L or in μg/L) before and after treatment, respectively. The results are the average of triplicate measurements, and the precision in most cases is close to $\pm 1.5\%$ (cf. Table VII).

Antimicrobial Tests

A solution or suspension of the tested monomers, polymers, and polymer- metal complexes [prepared bydissolving 400 µg/mL (w/v) in sterile DMSO] was poured aseptically in a well of 6 mm diameter made by a borer in the seeded agar medium. After transferring *via* pipetting the same volume in wells of all tested microorganisms, bacteria test plates were incubated at 37°C for 24 h and fungal test plates were incubated at 25°C for 48 h. The activities were expressed as inhibition zones (mm, diameter, as clear areas). The least concentration, which showed the inhibitory effect on any specific microorganism, was considered as the minimum inhibitory concentration (MIC) which was determined using streptomycin and Mycostatin (50 µg/mL) as the references.

RESULTS AND DISCUSSION

General

Some of the heterocyclic amines are selected to prepare *N*-heterocyclic acylamideas monomers two types of heterocyclic rings are used depending on the nature of heterocyclic ring. Type (1) include4-aminopyridine,2-aminopyrimidine-5-carbonitrile and 4-aminopyridazine as a π-deficient ring system. Type (2) include 2-aminobenzimidazole, 2-aminobenzthiazole and pyrazole as a π-excessive ring systems. A comparison study between these two types in the area of metal uptake and ion selectivity is aimed. π-Excessive ring systems are expected to be more efficient than that of π-deficient ring system because of the availability of electrons on the chelating center.

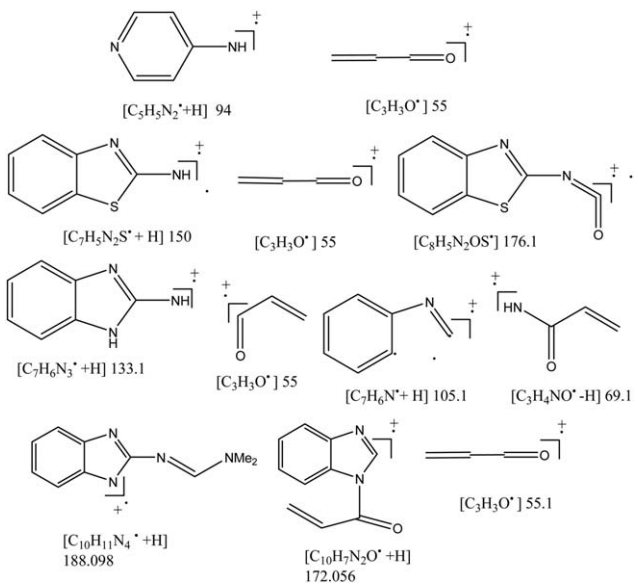

Scheme 4. Fragments pattern of mass spectra of monomers.

Table II. IR Δv (cm^{-1}) for PNBTA-M- Complexes

Assay	v_{NH}	Δv	$v_{C=O}$	Δv	$v_{C=N}$	Δv	v_{C-S}	Δv	Center of chelation	Complex form
PNBTA	3423		1697		1563		676			
PNBTA-Ni-complex	3422	1	1675	22	1586	3	663	13	CO & C—S	B
PNBTA-Cd-complex	3433	10	1665	32	1568	3	662	1	NH & CO	A
PNBTA-Fe-complex	3407	16	1682	15	1555	8	676	0	NH & CO	A
PNBTA-Pb-complex	3425	2	1651	46	1551	12	681	5	CO & C=N	C

Characterization of Monomers

Acryloyl chloride reacts with different amines in 1 : 1 molar ratioexcept in the case of 2-aminobenzimidazole reacted with 1 : 1 and 1 : 2 (amine : acryloyl chloride) molar ratio. The 1 : 1 ratio gave *N*-(1H-benzo[d]imidazol-2-yl)acrylamide (NBIA) with low yield while 1 : 2 ratio gave *N*-(1-acryloyl-1H-benzo[-d]imidazol-2-yl)acrylamide (NABIA) and NBIA. However, monoacylated NBIA product was obtained in nonsignificant amount and it was observed only in the GC-MS data (cf. Scheme 1).

On the other hand, 2-aminobenzimidazole was reacted dimethylformamidedimethylacetal (DMFDMA) to block the amino group and gives *N′*-(1H-benzo[d]imidazol-2-yl)-*N,N*-dimethylformamidine (BIDMF). The latter reacted with acryloyl chloride to give the target mono acylatedmonomer,*N′*-(1-acryloyl-1H-benzo[d]imidazole-2-yl)-*N,N*-dimethylformamidine (ABIMF).

In addition, 3-methyl-1H-pyrazol-5(4H)-one reacted with acryloyl chloride to give 1-acryloyl-3-methyl-1H-pyrazol-5(4H)-one (AMP) (Scheme 2).

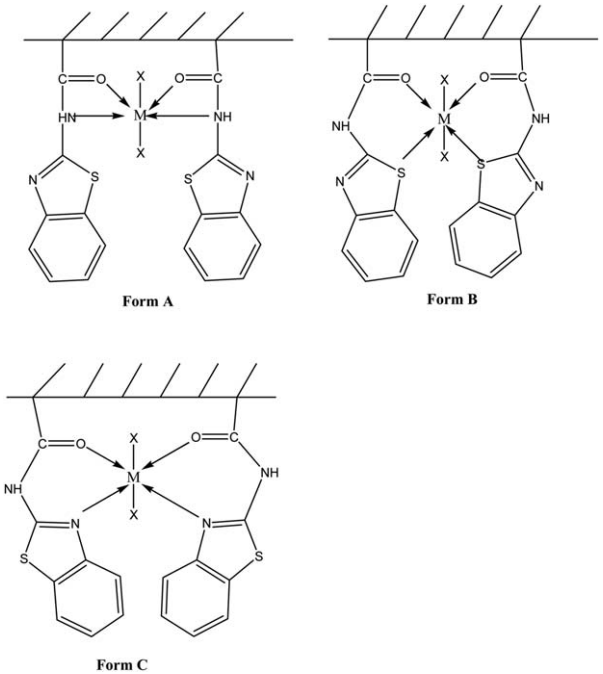

Scheme 5. Complexation forms of PNBTA with different metals.

The structure of the monomers was established using elemental analysis and spectral data. Trials to prepare *N*-(5-cyanopyrimidin-2-yl)acrylamide and *N*-(pyridazin-4-yl)acrylamide from 2-aminopyrimidine-5-carbonitrile and 4-aminopyridazine, respectively, are failed. This may be because of the π-deficient of the heterocyclic ring and delocalization of lone pairs of electrons of the amino nitrogen atom with heterocyclic rings.

All the prepared monomers were transferred to the corresponding polymers *via* heating the monomer solution in DMF with ABIN at 75°C (Scheme 3).

Mass Spectra of the Prepared Monomers

Table I showed the mass spectra of monomers and their elemental analysis. The mass spectrum of NPA showed $m/z = 148$ (4%) and its fragments are at 94.1 (100% base peak) and 55.0 (18%). The NBTA showed m/z at 204.1 (42%) and fragments at 176.1 (100%, base peak), 150.1 (28%), and 55.1 (14%). The NBIA showed m/z at 187.1, (60%) and fragments at 133.1, 105.1, 69.1, and 55.1, while GC MS of NABIA showed retention time at 4.57 and 7.19 with m/z 187.1 and 241.2, respectively. The ABIMF showed m/z at 242.12 (15%) and fragments at 188.1, 172.1, and 55.1. The expected structure of the fragment

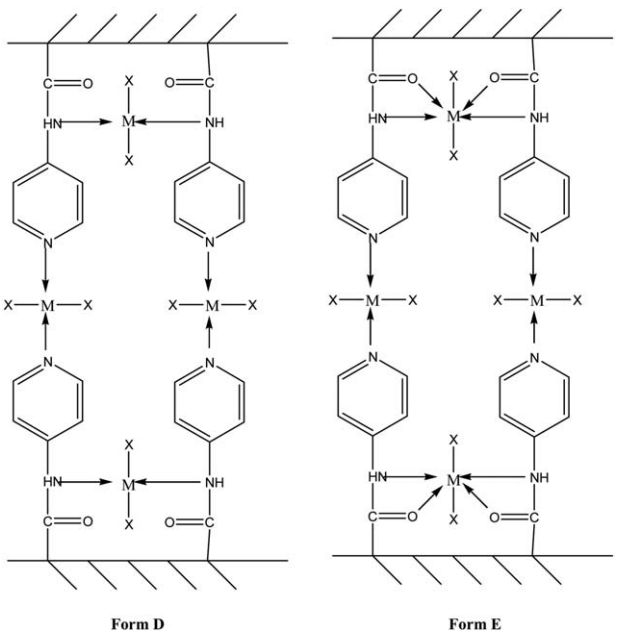

Scheme 6. Complexation forms of PNPA with different metals.

Table III. IR Δv (cm^{-1}) for PNPA-M- Complexes

Assay	v_{NH}	Δv	$v_{C=O}$	Δv	$v_{C=N}$	Δv	Center of chelation	Complex form
PNPA	3320		1659		1540			
PNPA-Cd-complex	3226	94	1656	3	1560	20	NH, C=N	D
PNPA-Fe-complex	3397	77	1633	26	1556	16	CO, NH & C=N	E
PNPA-Pb-complex	3441	121	1665	6	1569	29	NH, C=N	D
PNPA-Cu-complex	3221	99	1654	5	1572	32	NH & C=N	D

pattern for NPA, NBTA, NBIA, and ABIMF are shown in Scheme 4.

NMR (^1H and ^{13}C) Spectra

The ^1H NMR spectra of the monomers were recorded for d_6-DMSO solutions in absence and presence of D_2O. The spectrum of NPAexhibits a broad signal at δ 6.66 which disappeared on adding D_2O assigned to the NH protons. The low field position and shape of this signal could be referred to the participation of the NH protons in hydrogen bonding. The pyridine-H appeared at δ 8.16, 8.14 (d, 1H, $J = 6.4$ Hz); 8.01, 7.99 (d, 1H, $J = 5.6$ Hz); 6.80, 6.78 (d, 1H, $J = 6.4$ Hz), and 6.56, 6.55 (d, 1H, J=5.6 Hz). The peaks at δ 6.93, 6.91, and 5.86, 5.84 are assigned to the ethylenic protons.

The ^1H NMR spectrum of NBTA reveals the presence of NH at δ 10.56 which disappeared on adding D_2O. The aromatic protons appeared at δ 7.93, 7.92 (d, 1H, J=5.2), 7.86, 7.84 (d, 1H, $J = 5.6$ Hz), 7.60 (t, 1H, $J = 5.6$ Hz), 7.46 (t, 1H, J=5.2 Hz). The ethylenic protons, $=CH_2$, appeared as doublet at δ 5.75 and 6.22 ppm.

The ^1H NMR of NBIA showed the presence of NH at δ 6.40 ppm (D_2O-exchange). The aromatic protons appeared at δ 7.43–6.86 (m, 4H, aromatic–H). The ethylenic protons appeared at δ 5.75 and 6.22 ppm. On the other hand, ^1H NMR of NABIA showed peaks at 7.69, 7.39–6.96 and 6.12, 5.70 ppm assigned to NH, aromatic-H and ethylenic protons, respectively. The ^{13}C NMR of NBIA showed peaks at 169.43, 154.63, 137.06, 132.95, 121.42, 117.25, and 111.53 ppm. On the other hand, NABIA showed peaks at 169.43, 154.63, 148.30, 137.06, 132.95, 121.42, 120.76, 117.25, and 111.53 ppm.

2-Aminobenzimidazole reacted readily with DMFDMA to give N′-(1H-benzo[d]imidazol-2-yl)-*N,N*-dimethylformamidine which reacted with acryloyl chloride to give N′-(1-acryloyl-1H-benzo [d]imidazol-2-yl)-*N,N*-dimethylformamidine (ABIMF) (Scheme 2). The ^1H NMR reveals the presence of imine and aromatic proto ns at 9.01 and 7.40, 7.24 ppm, respectively. Ethylenic protons appeared at 6.31, 5.28 ppm, in addition to methyl protons at 2.50 ppm. ^{13}C NMR showed bands at 160.28, 154.57, 141.23, 138.52, 135.26, 130.94, 123.16, 121.45, 111.86, 34.73 ppm.

Characterization of Polymers and their Metal Complexes

IR Spectra of Monomers and Polymers. The IR spectra of NPA; NBTA; NBIA; poly-*N*-(pyridin-4-yl)acrylamide (PNPA); poly-*N*-(benzo[d]thiazol-2-yl)acrylamide (PNBTA) and *poly-N-(1H*-benzo[d]imidazol-2-yl)acrylamide (PNABIA)] as well as their complexes were recorded as KBr discs. The main bands of their tentative assignments are described as:

The spectrum of NPA displayed bands at 3336 and 3190 assigned to υ(NH) and —CH=CH_2, respectively. Also, the spectrum exhibits a very strong band at 1654 due υ(CO) of the amide group. This band appeared at 1659 cm^{-1} in the corresponding polymer. The band at 1593 is assigned to —CH=CH_2 which is not observed in the spectrum of its corresponding polymer (PNPA) indicating the polymerization *via* —CH=CH_2. This also confirmed from the disappearance of the band at 3190 cm^{-1} in the monomer.

The spectrum of NBTA showed bands at 3370, 3291, and 1648 cm^{-1} assigned to NH, —CH=CH_2 and υ(CO), respectively. The amide band appeared at 1697 cm^{-1} in the corresponding polymer. The disappearance of the strong band at 3050 cm^{-1}, in the monomer, characteristic of the —CH=CH_2 in PNBTA indicates the polymerization *via* —CH=CH_2.

The bands observed in the spectrum of NBIA at 3233, 3091, and 1648 cm^{-1} are because of NH, —CH=CH_2 and C=O. The —CH=CH_2 band is not observed in the spectrum of its corresponding polymer (PNBIA) indicating the polymerization via —CH=CH_2.

The IR spectrum of *N′*-(1-acryloyl-1H-benzo[d]imidazol-2-yl)-*N,N*-dimethylformamidine showed bands at 3060, 2978 and 2945 assigned for —CH—CH_2 and CH-aliphatic, respectively. The carbonyl group and —C=C— are appeared at 1650 and 1630 cm^{-1}, respectively. In addition, the band at 1562 is assigned to —CH=CH_2 and not observed in the spectrum of its corresponding polymer meaning that the polymerization takes place at —CH=CH_2.

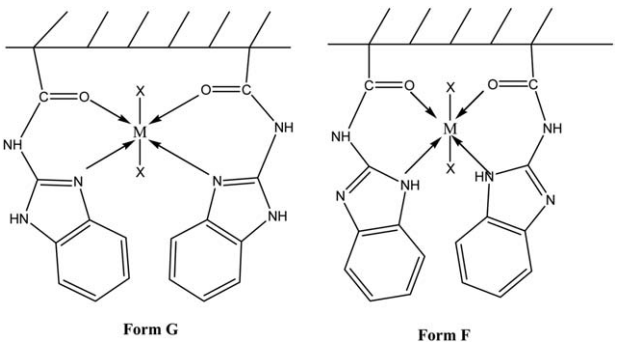

Scheme 7. Complexation forms of PNABIA with different metals.

Table IV. IR Δv (cm^{-1}) for PNBIA-M- Complexes

Assay	v_{NH}	Δv	$v_{C=O}$	Δv	$v_{C=N}$	Δv	Center of chelation	Complex form
PNBIA	3396		1650		1534			
PNBIA-Fe-complex	3405	9	1676	26	1538	4	NH & CO	F
PNBIA-Pb-complex	3438	42	1681	31	1539	5	NH & CO	F
PNBIA-Cd-complex	3343	53	1654	4	1577	43	NH & C=N	G
PNBIA-Cu-complex	3321	75	1651	1	1567	33	NH & C=N	G

Table V. Ion Selectivity of PNBTA Expressed in (ppm)

Metal ion	Before treatment (ppm)	After treatment (ppm)	Value of metal uptake (ppm)	% of metal uptake
Cu(II)	11,636.192	1934.2125	9701.9795	83.37
Ni(II)	16,294.215	1607.5567	14,686.6583	90.13
Pb(II)	57,459.441	5134.4644	52,324.9766	91.06
Cd(II)	26,046.321	2381.7751	23,664.5459	90.85
Fe(III)	13924.202	1150.0519	12,774.1501	91.74

Table VI. Ion Selectivity of PNPA Expressed in (ppm)

Metal ion	Before treatment (ppm)	After treatment (ppm)	Value of metal uptake (ppm)	% of metal uptake
Cu(II)	11,636.192	8699.2170	2936.9750	25.24
Ni(II)	16,294.215	15,088.4431	1205.7719	7.40
Pb(II)	57,459.441	52,753.5127	4705.9283	8.19
Cd(II)	26,046.321	24,744.0049	1302.3161	5.00
Fe(III)	13,924.202	10,711.8886	3212.3134	23.07

Metal Polymer Complexes. The synthesized polymers have different chelating centers such as C=O, NH, C—S of thiazole ring or C=N of thiazole or imidazole ring.

The different chelating forms (A-F) are assigned based on the IR data. Table II showed Δv of different group in comparing with that of polymer PNBTA. Thus, the IR of PNBTA-Cd complex showed Δv 10 and 32 cm^{-1} for NH and C=O, respectively. IR of PNBTA-Fe-complex showed Δv 16 and 15 cm^{-1} for NH and C=O, respectively. Accordingly, form A was assigned for these polymeric complexes. While form B assigned for PNBTA-Ni-complex where Δv 22 cm^{-1} for C=O group. Form C was assigned for PNBTA-Pb complex where Δv 46 and 12 cm^{-1} for C=O and C=N, respectively (Scheme 5).

The complexation of PNPA with Cd, Fe, Cu, and Pb ions may be assigned as indicated in Scheme 6. The IR of PNPA-Cd complex showed Δv 94 and 20 cm^{-1} for NH and C=N, respectively, while the IR of PNPA-Pb complex showed Δv 121 and 29 cm^{-1} for NH and C=N, respectively. In addition, the Δv values for NH and C=N in PNPA-Cu complex are 99 and 32 cm^{-1}, respectively (Table III). Accordingly, form D is

Table VII. ICP-OES Results of a Gulf Ocean Water Sample Before and After Treatment with the Chelating Polymer BNBTA

Metal ion	C_i	C_f	% of metal uptake
[a]Na^+	16,427.550	2506.550	84.742
[a]K^+	763.900	178.260	76.664
[a]Mg^{2+}	1611.400	164.580	89.787
[a]Ca^{2+}	509.500	16.870	96.689
[b]Co^{2+}	2.540	0.273	89.252
[b]Ni^{2+}	13.750	0.173	98.737
[b]Cu^{2+}	13.700	0.154	98.876
[b]Cd^{2+}	BDL	ND	ND
[b]Pb^{2+}	74.200	25.148	66.108
[b]Fe^{3+}	1.070	0.014	98.692
[b]Hg^{2+}	15.100	0.885	94.139

[a] Ci in mg/L.
[b] Ci in μg/L.
ND: not detected; BDL: below detection limit.

Table VIII. TGA of PNPA Metal Complexes

Polymer metal complex	TGA weight losses % and temperature (°C)
PNPA-Cd complex	6.46% at 63.55°C; 11.57% at 286.62°C; 19.89% at 385.98°C; 3.13% at 510.48°C and 6.98% at 695.46°C. Total loss is 48.24%. Residue of metal nitride is 51.75%.
PNPA-Fe complex	4.69% at 50.21°C, 10.93% at 185.39°C, 3.13% at 375.96°C, 0.42% at 450.62°C, 0.470% at 531.96°C and 0.98% at 749.65°C, 25.41% at 800.0°C. Total weight loss is 46.05%. Residue of metal nitride is 53.94%.
PNPA-Pb complex	5.10% at 266.76°C, 7.09% at 344.55°C, 0.34% at 623.88°C, 0.308% at 692.24°C and 15.15% at 800.0°C. Residue of metal nitride is 72.00%.

assigned for these polymeric complexes. Form E is assigned for PNPA-Fe complex where Δv of 77, 26, and 16 cm^{-1} for NH, CO, and C═N.

The structure of PNBIA complex with different metal ions was suggested as indicated in Scheme 7. The IR of PNBIA-Fe complex and PNBIA-Pb complex showed Δv 10 and 42 cm^{-1} for

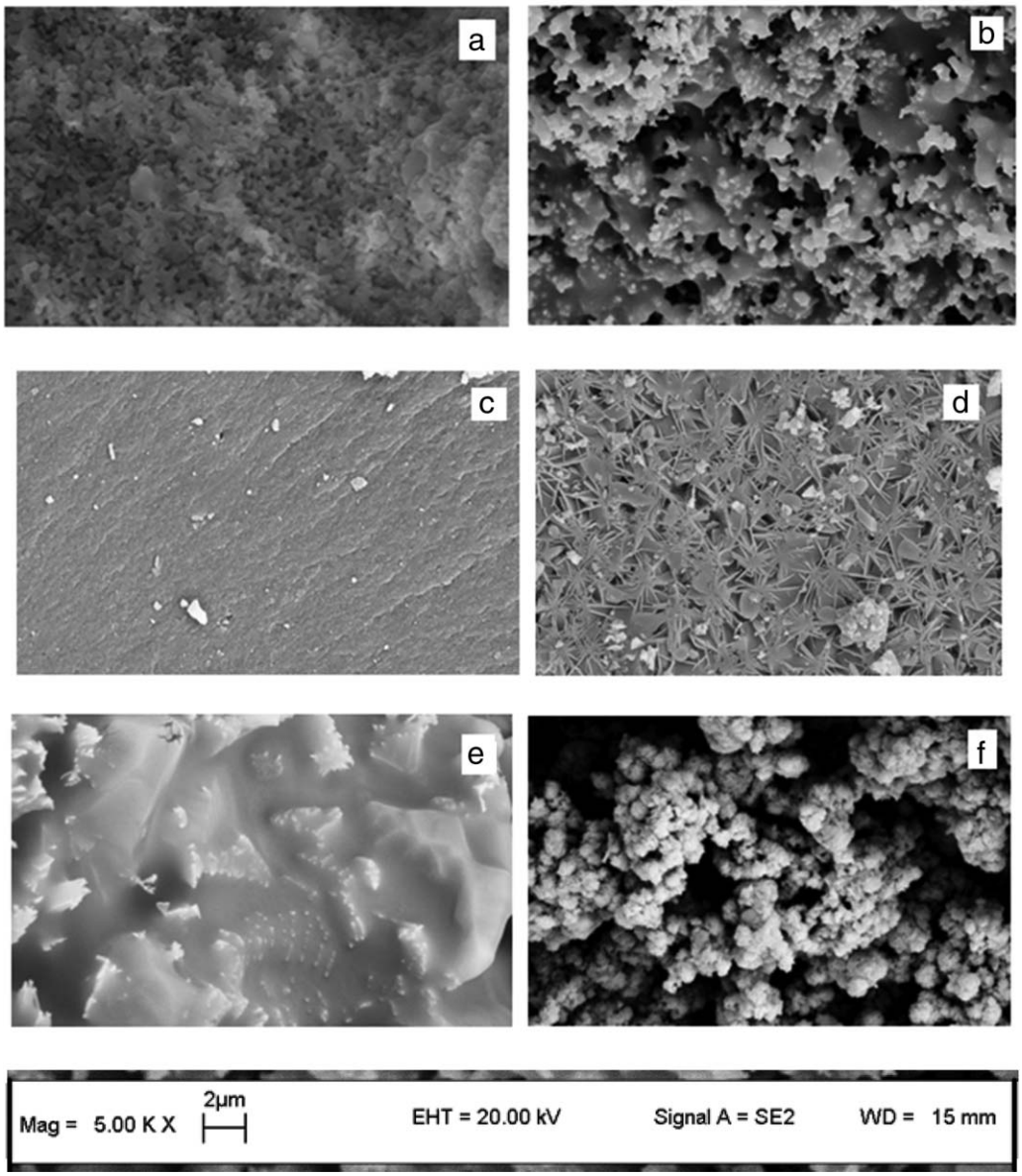

Figure 1. SEM micrograph of (a) PNPA; (b) PNPA-Cd complex; (c) PNPA-Fe complex; (d) PNPA-Cu complex; (e) PNBIA; (f) PNBIA-Cu complex.

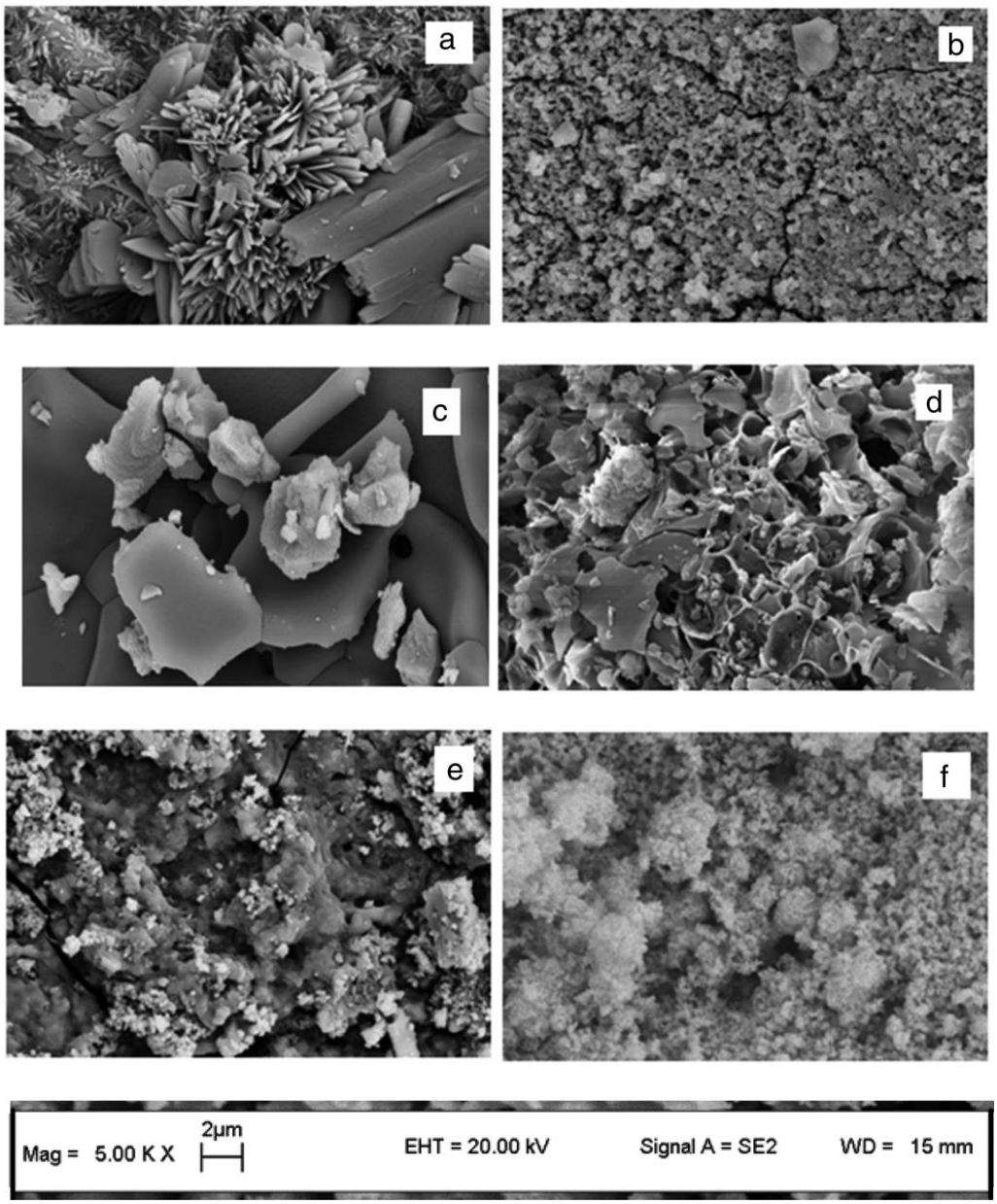

Figure 2. SEM micrograph of (a) PNBIA-Fe complex; (b) PNBIA-Cd complex; (c) PNBIA-Cu complex; (d) PNBTA; (e) PNBTA-Cd complex; (f) PNBTA-Pb complex.

NH, respectively. The carbonyl group showed values of 26 and 31 cm^{-1}, respectively (Table IV). Thus, form (F) is assigned for both structures. On the other hand, form G is assigned for PNBIA-Cd and PNBIA-Cu complexes, where Δv 53 and 75 cm^{-1} for NH and Δv 43 and 33 cm^{-1} for C═N.

Ion Selectivity

A mixture of different metal salts was treated with different polymers and the metal content of the blank solution and the solutions after treatment for 24 h with polymer was measured using ICP. The difference refers to the metal uptake value.

ICP of a mixture of metal nitrate (Cu^{2+}, Ni^{2+}, Cd^{2+}, Co^{2+}, Fe^{3+}, or Pb^{2+}) before and after treating with the polymer are measured by AAS and given in Table V. The polymer selectivity order could be arranged as follows:

Fe^{3+} (91.74%) > Pb^{2+}(91.06%) > Cd^{2+} (90.85%) > Ni^{2+} (90.13%) > Cu^{2+} (83.37%). On the other hand, Table VI showed the metal ICP of PNPA with mixture of different metal salt solution. The selectivity showed the following order:

Cu^{2+} (25.24%) > Fe^{3+} (23.07%) > Pb^{2+}(8.19%) > Ni^{2+} (7.40%) > Cd^{2+} (5.00%).

In the light of these data and the polymer-metal complexes discussion, the metal uptake by PNBTA is higher than PNBIA and PNPA, respectively. This may be because of the nature of dentate atoms in thiazole moiety with high electron density as a pi-excessive ring system and also the presence of soft sulfur atom

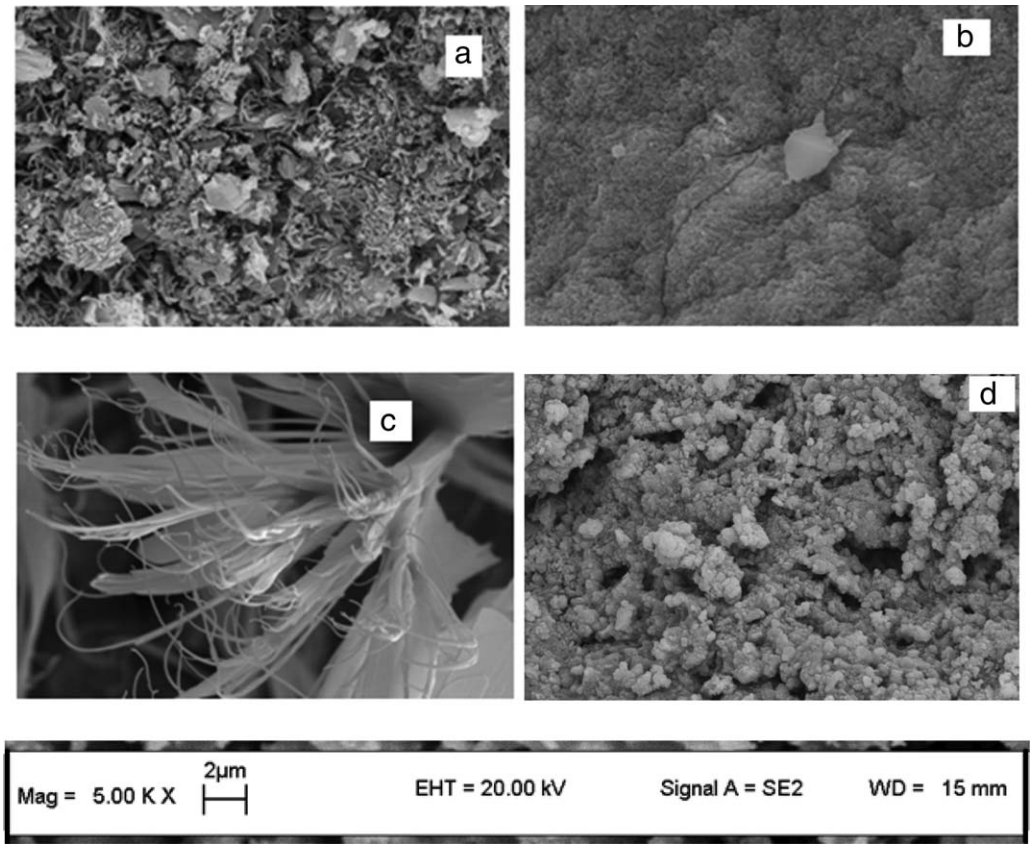

Figure 3. SEM micrograph of (a) PNBTA-Fe complex; (b) PNBTA-Ni complex; (c) PNBTA-Mg complex; (d) PNBTA-Cu complex.

preferred by some metal ions as compared by nitrogen atom in pyridine with low electron density because of delocalization of lone pair of nitrogen atom in pyridine ring (pi-deficient ring). Moreover, the PNBTA is highly selective to many ions e. g. Fe, Pb, Cd, and Ni ions while PNPA is selective only to Cu and Fe ions.

Determination of Metal Ions in Water Samples

PNBTA was able to uptake many metal ions (Na, K, Mg, Ca, Co, Ni, Cu, Cd, Pb, Fe, and Hg) from the Gulf Ocean water with different percentages (Table VII). The Cu, Ni, Fe, Hg, and Co ions were measured in μg/L, while Na, K, Mg, and Ca were measured in mg/L. The data of ICP-OES before and after treatments and the percent of metal uptake onto the chelating polymer are reported in Table VIII and computed according to the following equation;

$$\%\ \text{srption} = \left[C_i - C_f / C_i\right] \times 100$$

where C_i is the initial concentration and C_f final concentration of the metal ions (mg/L or in μg/L) before and after treatments.

Structure and Morphological Investigation

In general, the change in the surface morphology may be attributed to the introduction of the metal ions in the polymer matrix. SEM was studied to confirm the chelation of the metal ions with the polymeric chain and to study how the change of surface occurred. The morphologies of PNPA and its metal polymer complexes with Cd^{2+}, Fe^{3+}, Pb^{2+}, and Cu^{2+} are shown in Figure 1, with 5000 magnifications. It is observed that the crystallinity of the metal complexes of PNPA-Cd complex, PNPA-Cu complex and PNPA-Pb complex is more than that of the polymer. This means chelation occurred on the surface of the polymer. In case of PNPA-Fe complex, smooth surface with scattered crystal on the surface was observed, may be because of the penetration of the metal ion. The higher crystallinity of the Pb^{2+}, Cd^{2+}, and Cu^{2+}complexes over the others could be attributed to the stronger embedding of metal ions in the matrix of the polymer than the others. Furthermore, the crystallinity of the complexes is as follows: $Pb^{2+} > Cd^{2+} > Cu^{2+} > Fe^{3+}$.

The morphologies of PNBIA and its metal polymer complexes are shown in Figure 1(e,f) and Figure 2(a–c). The SEM of PNBIA showed a cloudy surface. It is observed that the crystallinity of PNBIA-Fe complex (flower shape), PNBIA-Pb complex and PNBIA-Cu complex is more than that of the polymer. In case of PNBIA-Cd complex, a cracking in the surface was observed. The higher crystallinity of the Fe^{3+}, Pb^{2+}, and Cu^{2+} complexes over the others could be attributed to the stronger embedding of Fe^{3+}, Pb^{2+}, and Cu^{2+} in the matrix of the polymer than the others. These ions may be more fit with the polymeric cavities. Furthermore, the crystallinity of the complexes is: $Fe^{3+} > Pb^{2+} > Cu^{2+} > Cd^{2+}$.

The SEM of PNBTA and its metal polymer complexes are shown in Figure 2(d–f) and Figure 3(a–d). The SEM of PNBTA showed that the crystallinity of PNBTA-Mg complex (marine

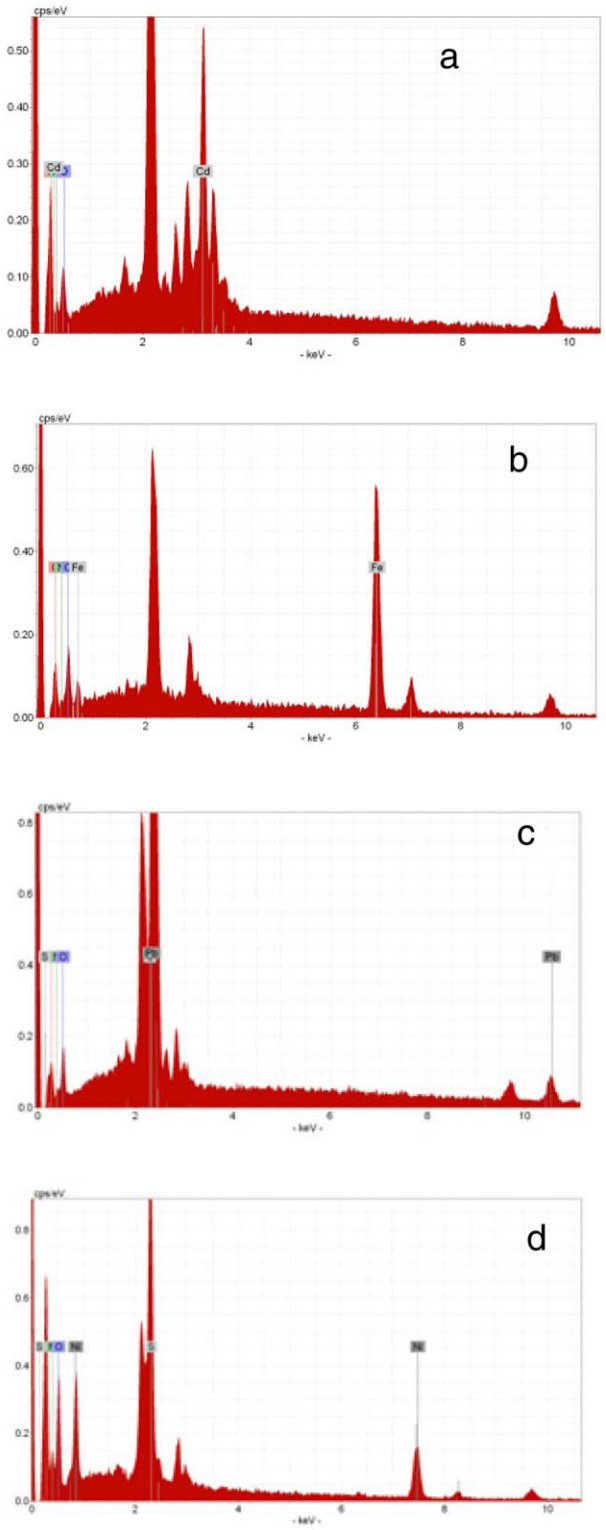

Figure 4. EDS of (a) PNPA-Cd complex; (b) PNPA-Fe complex; (c) PNBTA-Pb complex; (d) PNBTA-Ni complex. [Color figure can be viewed in the online issue, which is available at wileyonlinelibrary.com.]

organism shape). Moderate to low crystallinity was observed with PNBTA-Cd, PNBTA-Fe, PNBTA-Pb and PNBTA-Cu complexes as compared by original polymer depending on the nature of metal ion and change in the surface of the polymeric chain. In case of PNPA-Ni complex, a cracking sandy shape surface was observed.

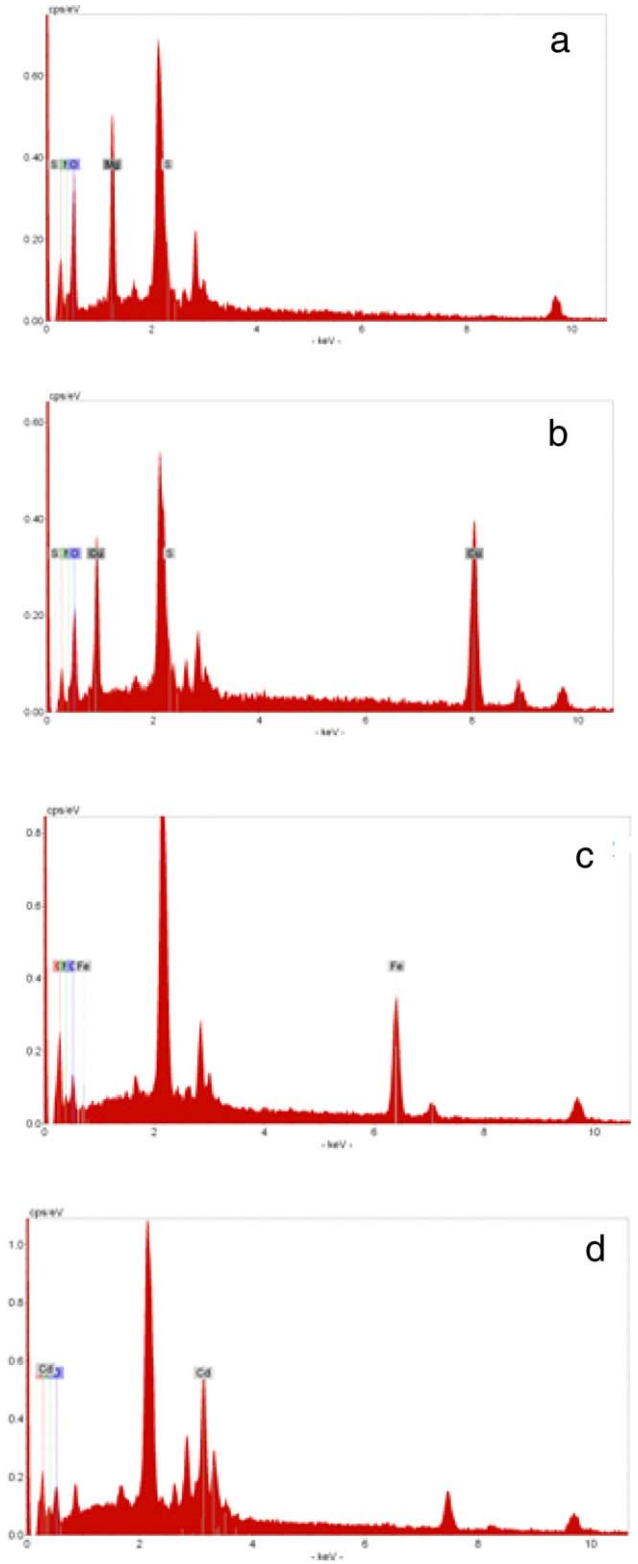

Figure 5. EDS of (a) PNBTA-Mg complex; (b) PNBTA-Cu complex; (c) PNBIA-Fe complex; (d) PNBIA-Cd complex. [Color figure can be viewed in the online issue, which is available at wileyonlinelibrary.com.]

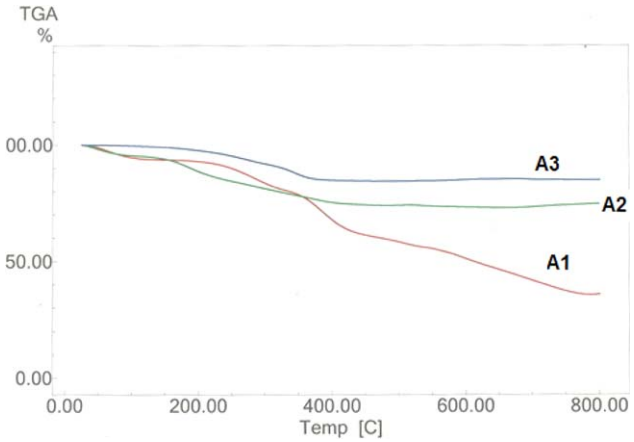

Figure 6. TGA of (A1) PNPA-Cd; (A2) PNPA-Fe and (A3) PNPA-Pb. [Color figure can be viewed in the online issue, which is available at wile yonlinelibrary.com.]

Energy Dispersive Spectroscopy (EDS)

EDS or EDX is an analytical technique used for the metal analysis or chemical characterization of a sample. This technique was used to analysis and confirms the presence of metal ions especially the instrument used for elemental analysis showed only the C, H, N, and S atoms. Figures 4 and 5 showed the EDX of selected metal complexes of PNPA, PNBIA, and PNBTA. The metal uptake by PNPA, PNBTA, and PNBIA has been confirmed by EDS spectra which reveal the presence of the different metal ions. Figure 4 showed the EDS spectra of PNPA-Cd, PNPA-Fe, PNBTA-Pb, and PNBTA-Ni complexes. Moreover, Figure 5 showed the EDS of PNBTA-Mg, PNBTA-Cu, PNBIA-Fe, and PNBIA-Cd complexes. All EDS analyses confirm the presence of the metal ions in addition of other atoms, which confirm the metal uptake by different used polymers.

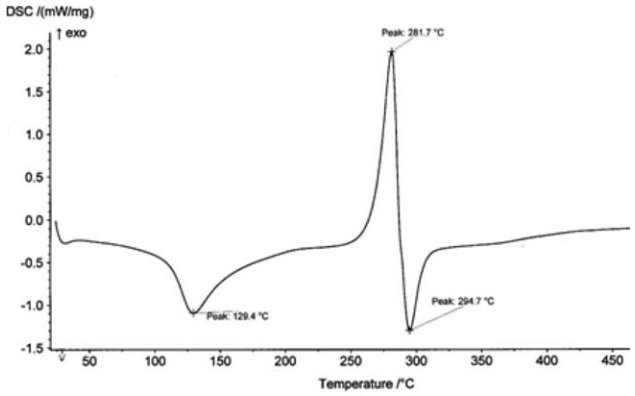

Figure 7. DSC of PNBTA-Ni complex.

Thermogravimetric Analysis (TGA) and Differential Scanning Calorimetry (DSC)

The thermogravimetric analysis (TGA) reflects the stability of polymer against temperature. High bond strength in the main chain, yielding of free radical, resonance stability, and polybinding are the most important requirements for polymers possessing high thermal stability. The heterocyclic polymers generally showed a low thermal stability because of the low bond strength between the carbon atom and the heteroatom, in addition, the loss of small particles and allowing of fragmentation in the polymeric chain.

The TGA of PNPA and its metal polymer complexes are investigated (*cf.* Figure 6). The weight loss (wt %) for the polymer and its metal polymer complexes at 25–200°C is because of the loss of water absorbed or adsorbed within the polymeric structure and also may be because of the inter- and intra-molecular H-bonding in the polymeric material.

The TGA study of PNBIA and PNBTA did not record because these polymers and their complexes are unstable enough against

Table IX. DSC of Metal Complexes with PNPA, PNBTA and PNBIA

Polymer metal complex	Temperature (°C)
PNPA-Cd complex	T_g 45°C, the onset 100°C, melting at 123.5°C and offset at 175°C. Crystallization at 309.4°C, oxidation of decomposition at 350–400°C.
PNPA-Fe complex	Melting at 148.0°C and crystalline at 220.3°C.
PNPA-Pb complex	Melting at 187.1°C and oxidation of decomposition at 287.7°C.
PNBTA-Cd complex	T_g at 30.0°C, exothermic peak for crystallization at 267.6°C, and endothermic peak for melting at 426.9°C.
PNBTA-Fe complex	T_g at 95.0°C. Crystallization exothermic peak at 201.6°C, the melting endothermic peak at 468.0°C.
PNBTA-Ni complex	T_g at 29.0°C. Crystallization exothermic peak at 281.7°C; two endothermic peaks at 129.4°C and 294.7°C.
PNBTA-Mg complex	Three endothermic peaks at 160.6°C, 191.6°C and 422.2°C and exothermic peak at 247.4°C.
PNBIA-Fe complex	T_g at 98.0°C; Crystallization exothermic peak at 212.8°C and melting at 223.0°C.
PNBIA-Pb complex	Melting at 191.2°C Crystallization exothermic peak at 250.0°C. Oxidation of decomposition peak at 425–450°C.

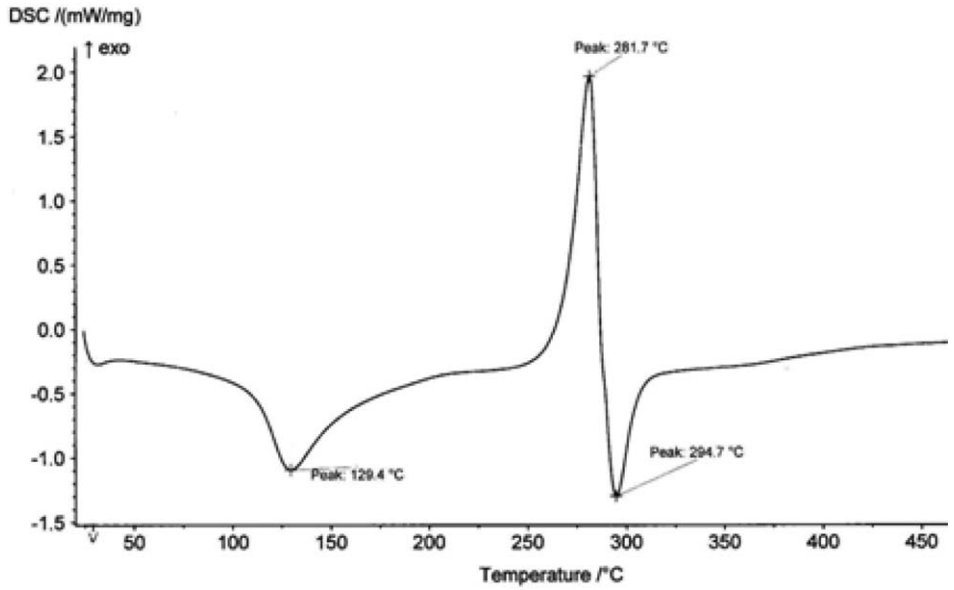

Figure 8. DSC of PNBIA-Pb complex.

heating. PNPA and its complexes showed data indicated the unstability over 800°C.

The data in Table VIII and Figure 6 reflect that the PNPA-Cd complex is thermally less stable than PNPA-Fe complex than PNPA-Pb complex this may be because of the nature of bonding between the metal and polymeric chain.

DSC means the measurement of the change of the difference in the heat flow rate to the sample and to the reference sample. DSC is used for examining polymeric materials to determine their thermal transitions. Study of DSC of the polymers containing heterocyclic moiety is interesting to observed thermal transitions. The study in a comparison between PNPA, PNBTA, and PNBIA metal complexes Table IX and Figures 7–9 reflect that the PNBTA showed higher melting followed by PNBIA and PNPA. High melting may be because of high molecular weight of a monomeric unit of PNBTA, PNBIA, and PNPA, respectively.

Antimicrobial Activity

The various biological activities of azole systems prompted us to study the antimicrobial activities of our newly synthesized products. The *in vitro* antibacterial activities of NPA, NBTA, NBIA, polymers, and complexes were evaluated against Gram positive and Gram negative bacteria (*S. aureus, B. subtilis, E. coli*, and *B. cereus*) and fungus (*Candida albicans*) are reported in Table X. The hole plate diffusion method was adopted for the activity measurements. The values recorded are the mean average for experiments repeated three times. Most of the tested

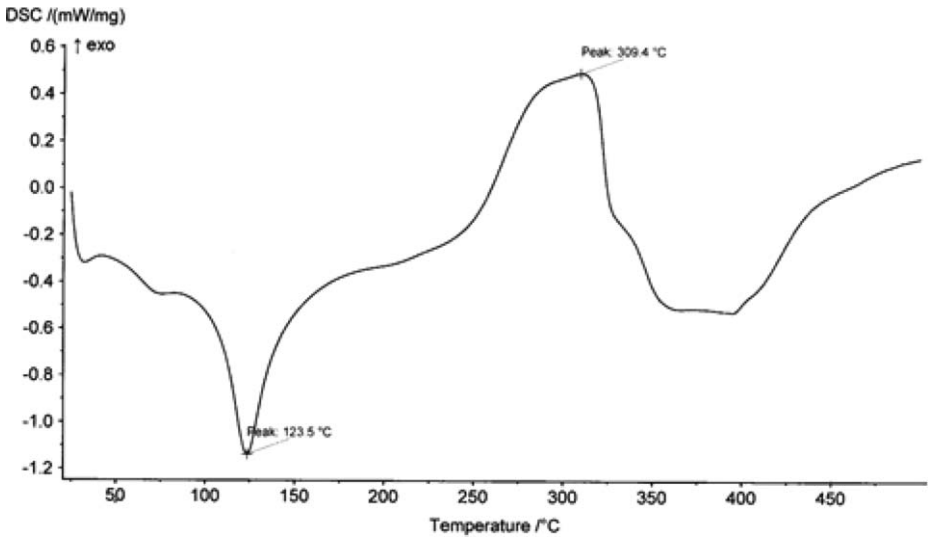

Figure 9. DSC of PNPA-Cd complex.

Table X. *In Vitro* Bactericidal and Fungicidal Activity of Some Newly Synthesized Compounds

Compd	*S. aureus*	*B. subtilis*	*E. coli*	*Salmonella*	*C. albicans*
NPA	++	++	+	+	+
NBTA	++++	+++	+++	++++	+++
NBIA	+++	++++	+++	++	+
ABIMF	+++	+++	++	+++	++
PNPA	++	+++	++	++	Nil
PNBTA	+++	++++	+++	++	+++
PNBIA	++++	+++	+++	+	+++
PNBTA-Pb-complex	+++	+++	++	+++	+
PNBTA-Ni-complex	+++	++++	+++	++	+++
PNBTA-Cd-complex	++	+++	+++	++++	++
PNBTA-Fe-complex	+++	++	++	+	++

++++ Severe effect (>30 mm); +++ Moderate effect (20–29 mm); + Slight effect (< 20 mm).

compounds showed a severe to moderate effect. Thus, severe effect against *S. aureus* was observed with the tested compounds except than that in case of NPA, PNPA, and PNBTA-Cd-complex showed a moderate effect. In case of *B. sublitis* NPA, PNBTA-Fe complex are showed a moderate effect while the other tested compounds have a severe effect. On the other hand, a severe effect of Gram-negative *E. coli* was detected with the tested compounds except ABIMF, PNPA, PNBTA-Pb, and PNBTA-Fe complexes which have a moderate effect. A slight effect was observed for NPA. NBTA, ABIMF, PNBTA-Pb, and PNBTA-Cd complexes have a severe effect against *Salmonella*, while NBIA, PNPA, PNBTA and PNBTA-Ni complex have moderate effect. A slight effect was observed with NPA, PNBIA and PNBTA-Fe complex. NBTA, PNBTA, PNBIA, and PNBTA-Ni complex showed a severe effect against *C. albicans* while, ABIMF showed a moderate effect. The other tested compounds showed a slight effect except PNPA which has no effect.

In the light of the above data, most of the tested compounds showed a severe to moderate effect this may be because of the presences of the heterocyclic moiety in the polymeric chain. On the other hand, the polymer containing thiazole ring has more effect against microorganisms than imidazole and pyridine rings. This can be rationalized because of the presence of thiazole moiety.

CONCLUSION

Polymers containing π-excessive heterocyclic ring are an advantage over that containing π-deficient in metal uptake and ion selectivity. All polymers showed a good to excellent effect against different tested microorganisms. Moreover, the polymer containing thiazole ring showed the high effect against different microorganisms as compared by that containing imidazole and pyridine rings. SEM study showed change in the surface of polymer as compared by polymer metal complex because of chelation of metal ions with different function groups on the surface of polymer and also because of the embedding of metal ions in the matrix of polymer. TGA showed low thermal stability because of the presence of heterocyclic moiety in the polymeric chain. Finally, DSC showed high melting for the polymer containing thiazole ring as compared by that containing imidazole or pyridine ring.

ACKNOWLEDGMENTS

The authors would like to acknowledge Kuwait University for the provision of grant No. SC 04/13 and the general facility projects grant Nos. GS 01/01 and GS 01/05.

REFERENCES

1. Montagna, L. S.; Catto, A. L.; Rossini, K.; Forte, M. M. C.; Santana, R. M. C. *AIP Conference Proceedings* **2014**, 1593(1, Proceedings of PPS-29, 2013), 329.
2. Khan, S. B.; Akhtar, K.; Seo, J.; Han, H.; Rub, M. A. *Chin. J. Polym. Sci.* **2012**, *30*, 735.
3. Rutkowska, M.; Krasowska, K.; Heimowska, A.; Adamus, G.; Sobota, M.; Musiol, M.; Janeczek, H.; Sikorska, W.; Krzan, A.; Zagar, E. *J. Polym. Environ.* **2008**, *16*, 183.
4. Lane, S. M.; Yom, J.; Kuang, Z.; Arifuzzaman, S.; Genzer, J.; Farmer, B. L.; Naik, R.; Vaia, R. A. *PMSE Preprints* **2009**, *101*, 920.
5. Kopeckova, P.; Pitt, C. G.; Habberfield, A. D.; Omelyanenko, V.; Kinstler, O.; Kopecek, J. *Proceedings of the International Symposium on Controlled Release of Bioactive Materials* **1996**, *23rd*, 869.
6. Etrych, T.; Jelinkova, M.; Rihova, B.; Ulbrich, K. *J. Control. Release* **2001**, *73*, 89,.
7. Rossi, F.; Ferrari, R.; Castiglione, F.; Mele, A.; Perale, G.; Moscatelli, D. *Nanotechnology* **2015**, *26*, 15602.
8. Henstock, J. R.; Rotherham, M.; Rashidi, H.; Shakesheff, K. M.; El Haj, A. *J. Stem Cells Transl. Med.* **2014**, *3*, 1363.
9. Xiang, T.; Wang, L.-R.; Ma, L.; Han, Z.-Y.; Wang, R.; Cheng, C.; Xia, Y.; Qin, H.; Zhao, C.-S. *Sci. Rep.* **2014**, *4*, 4604/1.
10. Mayur, K.; Ramesh, K.; Nitin, J.; Prashant, P.; Rajendra, G.; Jeevan, N. *J. Drug Deliv. Ther.* **2013**, *3*, 14.
11. Kanazawa, H. *Jpn. KokaiTokkyoKoho, JP* **2011**, *2011208133 A 20111020.*
12. Greiner, A.; Roecker, T. *PCT Int. Appl. WO* **2008**, *2008049250 A1 20080502.*
13. Petrie, E. M. *Rev. Adhes. Adhes.* **2014**, *2*, 253.
14. Shcharbin, D.; Shcharbina, N.; Bryszewska, M. *Recent Pat. Nanomed.* **2014**, *4*, 25.
15. Jiang, G.; He, G. *Mater. Des.* **2014**, *56*, 241.
16. Bal, T.; Murthy, P. N.; Sengupta, S. *Am. J. Pharm. Tech. Res.* **2013**, *3*, 271.
17. Du, W.; Zhou, H.; Luo, Z.; Zheng, P.; Guo, P.; Chang, R.; Chang, C.; Fu, Q. *Molecular Imprinting* **2014**, *2*, 18.

18. Seymour, M.; Reit, R.; Lund, B. R.; Voit, W. *Abstracts of Papers, 249th ACS National Meeting & Exposition, Denver, CO, United States,* **2015,** March 22–26, POLY-371.
19. Williams, K. R. *Abstracts of Papers, 249th ACS National Meeting & Exposition, Denver, CO, United States, March* **2015,** 22–26, (2015), POLY-74.
20. Figueiredo, L.; Santos, L.; Alves, A. *Adv. Polym. Technol.* **2015**, unpublished results.
21. Elassar, A.-Z. A.; Al Sughayer, A. H.; Al Sagheer, F. *J. Appl. Polym. Sci.* **2010**, *117*, 3679.
22. Elassar, A.-Z. A.; Al-Fulaij, O. A.; El-Sayed, A. E. M. *J. Polym. Res.* **2010**, *17*, 447.
23. Elassar, A.-Z. A.; El-Sayed, A. E. M.; Ahmed, F. S. *J. Appl. Polym. Sci.* **2010**, *117*, 200.
24. Al-Fulaij, O. A.; Elassar, A.-Z. A.; El-Dissouky, A. *J. Appl. Polym. Sci.* **2006**, *101*, 2412.